Chapter II

Miniaturized Paper Based Optical Micro-Device for the Monitoring of Creatinine

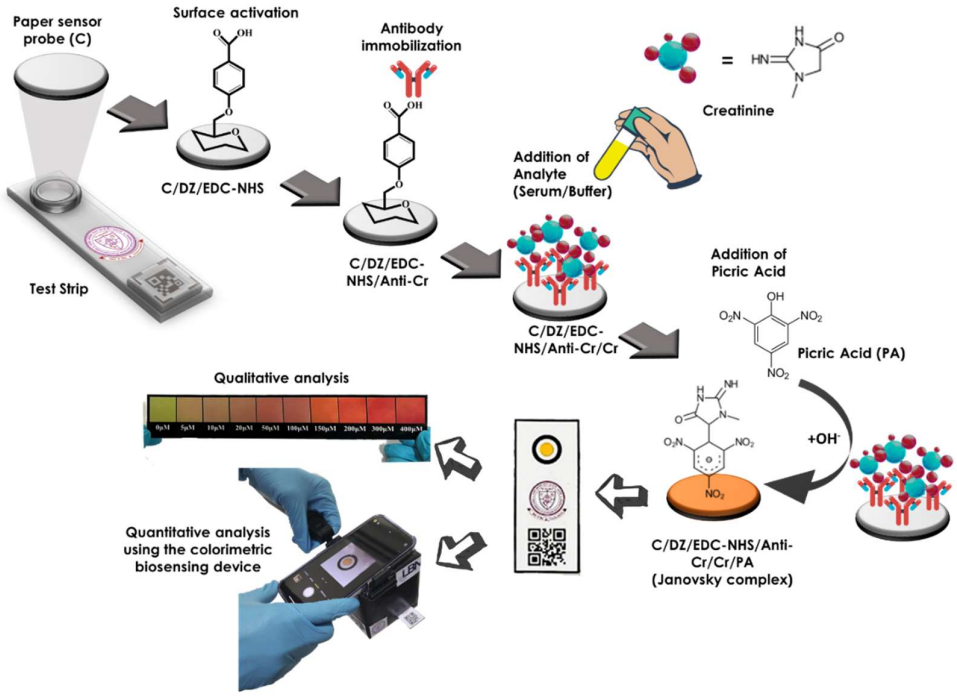

Divya et. al, *Biosensors, 2022, Vol 12,1118-1126* biosensors

1. Introduction

Chronic kidney disease has emerged as one of the most common conditions affecting more than 10% of the world's population, which counts to more than 800 million people. Over the last two decades, an exponential surge, i.e., a 42% increase in deaths caused by chronic kidney disease was recorded worldwide [1]. A study on the Global Burden of Disease shows that the surge in mortalities due to chronic kidney disease is emerging and becoming one of the major diseases leading to a global burden [2,3]. The divergence in prevalence and severity of chronic kidney disease is possibly due to the complex interaction between biological and non-biological risk factors. Therefore, diagnosing chronic kidney disease becomes tedious and important, especially targeting the more specific biomarker. In this critical condition, kidneys are not able to filter out the waste of natural atrophies from the body [4]. Usually, the kidney filters out the various nitrogen-based waste material and metals, including urea, uric acid, Creatinine, ammonium, and lead. Numerous biomarkers and bioanalytical tests for diagnosing renal diseases includes; albuminuria, serum Creatinine, Creatinine clearance, glomerular filtration rate, and the albumin-to-Creatinine ratio [5,6]. Most of the renal infections are diagnosed based on the presence of various biomarkers in extracellular fluids [7], however most of them are also related with several other pathological conditions [8]. Some bioanalytical tests, especially glomerular filtration rate are affected by age, gender, and lifestyle [9]. Therefore, selecting biomarkers is also one of the major criteria for properly diagnosing kidney disease. Serum Creatinine is a more specific biomarker preferred by medical practitioners for kidney damage globally [10]. Creatinine is a metabolic product of creatine phosphate produced by a nonenzymatic reaction and its excretion is the major indication of the state of kidney function [11]. The Creatinine released in human blood and urine is critically important to the kidney, thyroid, and muscular functions [12,13]. Creatinine concentration in serum is not influenced by protein intake, so the level of Creatinine in serum act as a more suitable and

effective indicator of kidney health. The normal physiological level of Creatinine in blood serum lies in the range of 45 - 140 μM, and it further exceeds in different diseased conditions [14]. The routine laboratory test for chronic kidney patients is mostly urine analysis indicating the presence of albumin/protein in the urine. Even the amount of microalbumin is considered a serious renal infection but is also associated with urinary tract infection. Also, in the urine analysis, urinary sediments such as hyaline casts, specific gravity, the color of urine, and/or muddy brown casts are considered equally important [15,16]. Apart from urine, blood urea nitrogen and Creatinine concentration tests are also recommended, which require long hours for testing and thus are not feasible for rapid, on-site detection. Many researchers have attempted to develop sensors based on various transduction systems for the detection of Creatinine using various methods, i.e., optical [17,18], electrochemical [19,20], and chromatographic techniques [21,22]. Apart from the optical system, other methods require expensive and dedicated instruments and skilled personnel to perform the analysis, so they are not very handy for the routine analysis [23,24]. In addition, optical sensors show an edge, especially in the medical field, because they can provide vital and complementary information without requiring laborious efforts. The most common optical methods for Creatinine detection are based on Jaffe's reaction [25] or enzymatic reaction [26]. The optical sensors relying this reaction are majorly performed in solution phase and does not utilize bioreceptors such as antibodies or aptamers [25]. Not only this the analysis in solution phase may also compromised when the target is present in real samples i.e., serum, urine, or other extracellular fluids [27]. The problem with such optically developed system is mainly related to its selectivity. Hence, engineering of a specific bioreceptor on to a solid surface can be utilized to develop a selective sensor system. Among various surfaces, paper-based matrix is the most simplistic one and has been greatly utilized to fabricate various types of biosensors [28–30].

Thus, we attempted to incorporate the Anti-Cr antibody on to the paper surface that makes the reaction more selective and sensitive. Although few attempts were made to develop a lateral flow assay-based kit for Creatinine detection, especially for kidney patients, in such a system, there is a chance of interruption in the flow of the target analyte due to the profusion of pores [28,31]. This issue has been examined and resolved by using the paper disc in which no sample movement is required, thus offering an edge over another system [28]. The paper-based systems are more commercially viable, easy to use, and environmentally suitable. Conventionally the optical signatures are subjected for Red/Green/Blue (RGB) analysis, that depends on the changing intensities of these colors. These change in color intensities helps to obtain the calibration plot for an analyte detection associated with diverse biomolecular and chemical reactions [32,33]. Hence, the relationship between such change in color and analyte concentration needs to be established for quantitative detection of Creatinine.

In this work, we have developed a hand-held, on-site, miniaturized, point-of-care diagnostic device for the sensitive and quantitative detection of Creatinine in serum samples which is related with the renal disease condition. A cellulosic filter paper was selected as a probe material on which the sensor surface was constructed. The sensor surface was fabricated through chemical modifications and antibody immobilization for the specific and sensitive Creatinine measurement. Further, the fabricated probe was thoroughly characterized using Fourier transform infrared spectroscopy (FTIR), atomic force microscopy (AFM), and controlled colorimetric studies after each step, and assembled on a paper strip. As per our knowledge, this is a first of its kind attempt to fabricate a sensing probe using Anti-Cr antibody. After that, we designed a miniaturized Hardcase bound prototype of a device in which a dedicated imaging tunnel was constructed. The device is user-friendly and allows a user to capture the probe's image using a smartphone. The color condition and the color-changing phenomena indicating the proportional change in analyte concentrations were detected through

the developed device. The selectivity, real sample analysis, and reproducibility were also validated to establish the suitability of the overall sensing device's market potential and application in daily life.

2. Experimental Section

2.*1. Materials and Reagents*

All the chemical reagents were purchased from standard companies and further used without any purification steps. Deionized water was used to prepare the buffer solutions for the experiments following basic laboratory methods. Creatinine (Cr), sodium nitrite, o-nitrobenzoic acid, picric acid (PA), 1-(3 dimethylaminopropyl) 3-ethyl carbodiimide hydrochloride (EDC), n-hydroxysuccinimide (NHS), Na_2HPO_4, NaH_2PO_4, sodium chloride, serum albumin, lactose, citric acid, uric acid, and potassium chloride were procured from SRL India. Grade-1 Whatman filter paper was purchased from Whatman Inc., Merck-Millipore, USA. Standard Serum (RM 9955) and Tween-20 were procured from Hi-media, USA. Anti-Cr antibody (ab30719) procured from Abcam, Inc. 0.01M PBS (pH 7.4) and 0.01M PBS-Tween (pH 7.4; 1% tween) buffer were prepared using the standard method [34]. Diazonium salt was prepared by adding 184.5 mg o-nitrobenzoic acid, 130.0 mg sodium nitrite, and 36.0 mg ascorbic acid sequentially in 45.0 ml HCl (1M).

2.2. Designing of sensing probe

Grade 1 Whatman filter paper (C) was selected as the base material for the fabrication of the sensor probe. For this, a whatman filter paper was cut into circular disc form using a paper punching machine to have the defined diameter for all discs. After that, the discs were treated with 4-carboxybenzene diazonium (DZ) salt by soaking them for at least six hours. Then the discs were thoroughly washed using a sterile PBS solution forming the C/DZ surface. The disc's surface (C/DZ) was further treated with EDC/NHS (140 - 100 mM, freshly prepared), which helps activating the carboxyl groups on the C/DZ surface, forming the C/DZ/EDC-NHS

surface. After washing, the Anti-Cr (1.7 µg/µL) antibody was immobilized over the C/DZ/EDC-NHS surface. The immobilization occurred because of the reaction between the amino groups of the Anti-Cr antibody and carboxyl groups on the modified C/DZ/EDC-NHS surface. After this step, the developed probe was presented as C/DZ/EDC-NHS/Anti-Cr. Finally, to avoid false positive signal generation and minimize nonspecific interaction, the surface (C/DZ/EDC-NHS/Anti-Cr) was treated with 1% BSA for 30.0 mins. This step is further completed by washing the probe with autoclaved PBS-Tween for about 1.0 min to remove unabsorbed BSA. The fabrication step of each layer was confirmed by different techniques, i.e., FTIR and AFM, and optical techniques. **Figure 2.1** illustrates the detailed step-by-step sensor probe fabrication method and the proposed colorimetric sensing device.

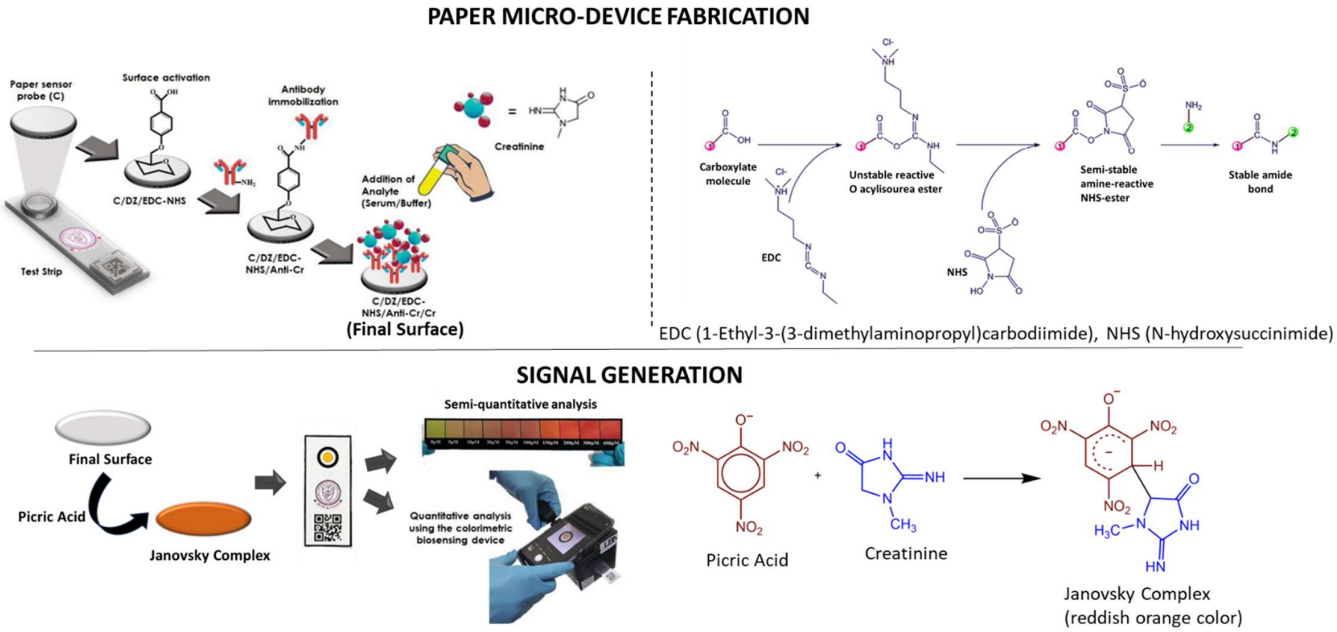

Figure 2.1: *Illustration of the step-by-step fabrication of the sensor probe and the signal generation using the developed paper micro device*

2.3. C/DZ/EDC-NHS/Anti-Cr biosensor probe testing

Creatinine was determined through the reaction between the final sensing probe C/DZ/EDC-NHS/Anti-Cr and Creatinine forming C/DZ/EDC-NHS/Anti-Cr/Cr. To test the ability of the designed probe, different concentrations of Creatinine were utilized and allowed to react with

picric acid (PA) for 7.0 min (optimized). It was found that this reaction produces a reddish-orange colored complex catalyzed by Creatinine immunocomplexed to the C/DZ/EDC-NHS/Anti-Cr probe. The reaction between Creatinine and picric acid was also shown in the illustration (Figure 1). After that, the probe was assembled on a paper strip and fitted to the device prototype. A smartphone camera was used to record the color change of the probe in particular conditions followed by image processing. The quantification of color change was done by processing the corresponding RGB values of a specific color. The image processing was done in such a manner that a particular area was selected that specifically selects the colored probe area for analysis so that the error in RGB values and false positive results can be avoided during the imaging process. This area selection method also helps determine the accurate color intensity change by calculating the mean intensity of color in the uniformly distributed area.

The effective RGB intensities of the paper disc with color change were determined by using **equation 1**:

$$\boldsymbol{Effective\ I_{RGB}} = \mathbf{log_{10}} \frac{\boldsymbol{I_{RGB}(Blank)}}{\boldsymbol{I_{RGB}(Conc.)}} \qquad \textit{equation 1}$$

where, I_{RGB} represents the mean intensities of all primary color channels obtained from the selected area of PA-treated C/DZ/EDC-NHS/Anti-Cr/Cr probe surface.

3. Results and Discussions

3.1. Color channel selection

The image analysis was performed by following the RGB convention to assess the biosensing studies, where initially, the more efficient and sensitive primary color channel was chosen and examined. The data present in digital image analysis was determined in the form of effective I_{RGB}, which reflects the true pixel intensity of the color (reddish-orange color in this reaction). I_{RGB} consists of the intensities of three different principal color passages, which are represented as I_{Red}, I_{Green}, and I_{Blue}. The optical change shows the gradual change in the intensity of color

appearing and represents the complementary color absorption. Finally, to evaluate the analytical performance of the developed device depending upon the maximal change in sensitivity for the primary color channel, we performed a comparative analysis of all three primary color channels individually. **Figure 2.2 (a-d)** represents the change in color to reddish-orange in a time-dependent manner on the developed sensing probe and the complementary histograms in RGB and B manner at 0.0, 3.0, 5.0, and 7.0 minutes. After that, we focused on calculating the individual Effective $I_{Red,}$ Effective $I_{Green,}$ and Effective I_{Blue} in a time-dependent manner from 1.0 to 7.0 min. The obtained data were plotted with respect to changes in time as shown in **Figure 2.2 (e).** It was interesting to note that the highest signal change was observed for Effective I_{Blue} (0.1138 (± 0.0060) a.u./min), in comparison to the Effective I_{Green} (0.0619 (± 0.0024) a.u./min) and Effective I_{Red} (0.0248 (± 0.0039) a.u./min), which was also statistically significant ($p < 0.003; n = 3$).

Therefore, in all further sensing analyses, Effective I_{Blue} was considered as an analytical parameter calculated using **equation 2**

$$\boldsymbol{Effective\ I_{Blue} = \log_{10} \frac{I_{Blue}(Blank)}{I_{Blue}(Conc.)}} \qquad \textbf{\textit{equation 2}}$$

where, I_{Blue} represents the mean pixel intensity of the blue channel determined from the sensing probe C/DZ/EDC-NHS/Anti-Cr/Cr discs when treated with picric acid.

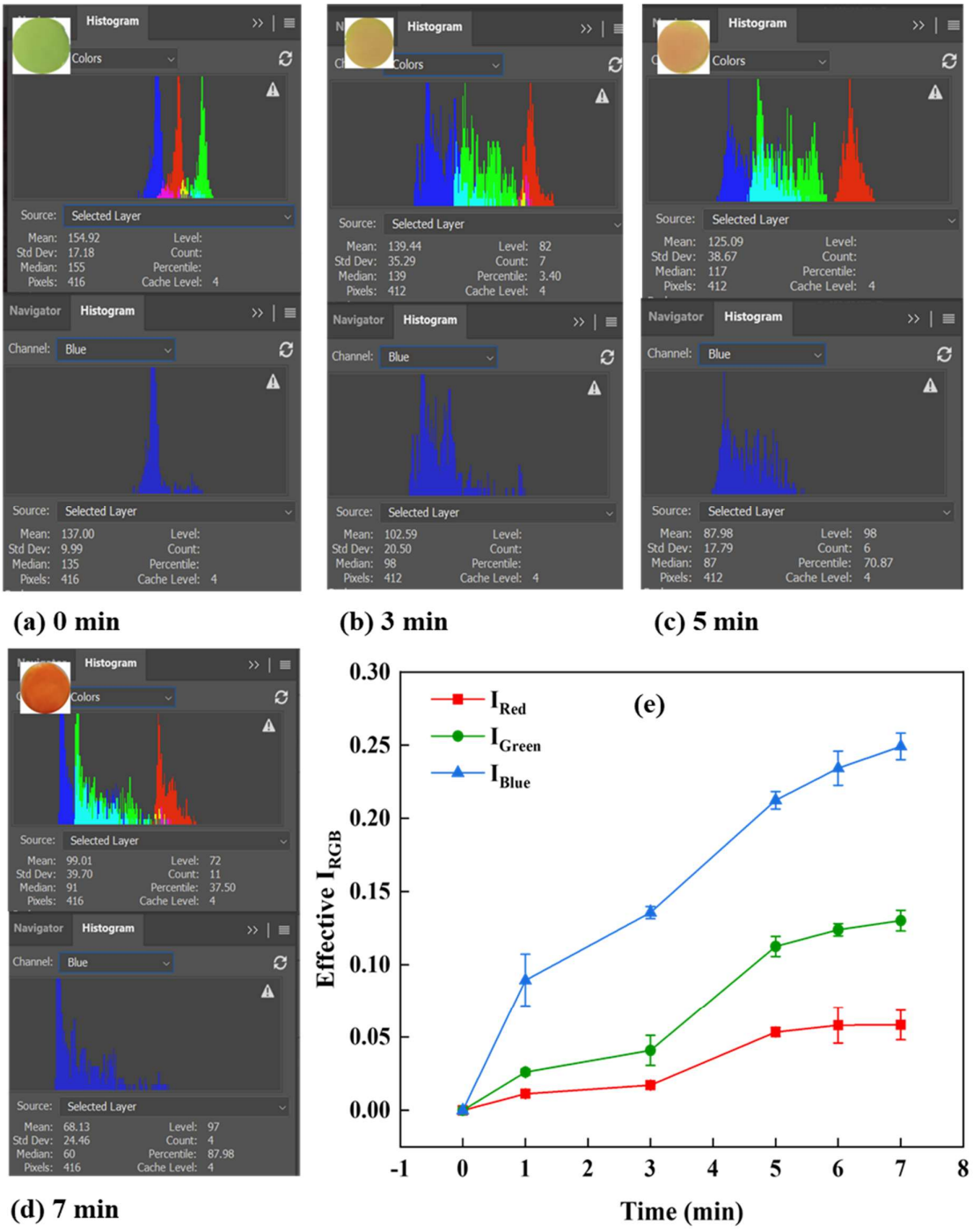

Figure 2.2: (a-d) *Histogram showing the change in color intensity along with the real image of disc showing real-time color change,* ***(e)*** *Representation of change of color intensity of all the three standards through RGB analysis, i.e., Effective* $I_{Red,}$ *Effective* $I_{Green,}$ *and Effective* I_{Blue}

3.2. Characterization of C/DZ/EDC-NHS/Anti-Cr/Cr probe

The developed sensing probe and the surface reactions were characterized step-by-step by various techniques, which includes optical analysis, FTIR, and AFM. Experiment showing the immunocomplexation formation was designed and performed to authenticate all the fabrication steps of the sensor probe. This study allowed the Creatinine to react with the final sensing probe, i.e., C/DZ/EDC-NHS/Anti-Cr/Cr, which was further washed and finally exposed with PA to form the reddish-orange color, which is represented in **Figure 2.3a(i).** We have characterized the different sensing probe surfaces to confirm and validate that the color change intensity was simply because of the immunocomplex formation and further the catalytic reaction between Creatinine and PA by conducting several control experiments. Such controlled experiments are extremely important to verify that the signals are not a false positive signal, but they are generated merely due to the Antigen-Antibody reaction. In the first controlled experiment, Creatinine was allowed to react with the Diazonium activated paper disc (C/DZ), which further interacts with the PA, developing the C/DZ/Cr/PA surface **(Figure 2.3a(ii))**. In this case the obtained Effective I_{Blue} value was found to be 0.024 (± 0.003), which was approximately 5 times lower compared to the final probe (**Figure 2.3a(i))**. In the next controlled experiment, Creatinine conjugated surface was examined which was not treated with PA (C/DZ/EDC-NHS/Anti-Cr/Cr) **(Figure 2.3a(iii))**. After examination the obtained Effective I_{Blue} value was found to be 0.018 (± 0.001), which was approximately 8.1 times lower compared to the final probe (**Figure 2.3a(i))**. whereas in another controlled study, Creatinine was not added to the sensing probe, but the probe was allowed to react with PA (C/DZ/EDC-NHS/Anti-Cr/PA) **(Figure 2.3a(iv)).** In this case the Effective I_{Blue} value was found to be 0.0022 (± 0.0001), which was approximately 53.2 times lower compared to the final probe (**Figure 2.3a(i))**. From the obtained controlled data negligible signals were obtained hence, the

fabricated sensor doesn't generate any false positive results. These results were statistically evaluated by t-test where the p-value was obtained to be $< 0.02; n = 3$.

Further, the design of the sensor probe was also confirmed through layer-by-layer characterization of the probe by FTIR. The FTIR spectra for the untreated cellulose paper (C) disc, the cellulose paper surface treated with diazonium substrate (C/DZ), the diazonium-activated paper surface with EDC-NHS (C/DZ/EDC-NHS), and the antibody immobilized final sensing surface (C/DZ/EDC-NHS/Anti-Cr) have been shown in **Figure 2.3 (b).** Representative peaks appeared between 1000 and 1200 cm^{-1}, 2995 cm^{-1}, and 3275 cm^{-1} because of the vibrations of C-C-C and C-O-C, and stretching vibrations of C-H and O-H, respectively in case of C **(Figure 2.3b(i))**. After this, the discs were treated with diazonium solution and the peaks are represented in **Figure 2.3b(ii).** Here the peaks appeared at 1700 cm^{-1} and 1515 cm^{-1}, which complements the C=O group and C=C group, respectively. These peaks are probably because of the introduction of carboxybenzyl flanking groups on the surface of the cellulose paper that leads to the formation of C/DZ surface. In the third step, the discs were allowed to react with EDC/NHS over the modified C/DZ surface where two sharp peaks of amide I and amide II at 1643 cm^{-1} and 1552 cm^{-1} were observed, respectively (**Figure 2.3b(iii))**. These peaks indicate that the bending vibrations of amide bonds formed when they were allowed to be coupled with NHS and carboxybenzyl flanking groups on the surface. These EDC/NHS-modified cellulose surface peaks in the FTIR spectra have also been recorded previously [29]. Finally, in the last step, the Anti-Cr was immobilized on the paper surface to form the final sensing probe, i.e., C/DZ/EDC-NHS/Anti-Cr, which was confirmed by the presence of two specific bands of amide I and amide II visible in **Figure 2.3b(iv).** However, after modification with Anti-Cr the amide I and II peaks were slightly shifted from their position as found on the EDC/NHS modified surface [35]. These observed stretching vibrations are the direct indications of the backbone conformation of the protein (Anti-Cr), which indeed

demonstrate the presence of immobilized Anti-Cr on the paper surface. Each layer was also characterized with reference to the thickness and surface topology using AFM.

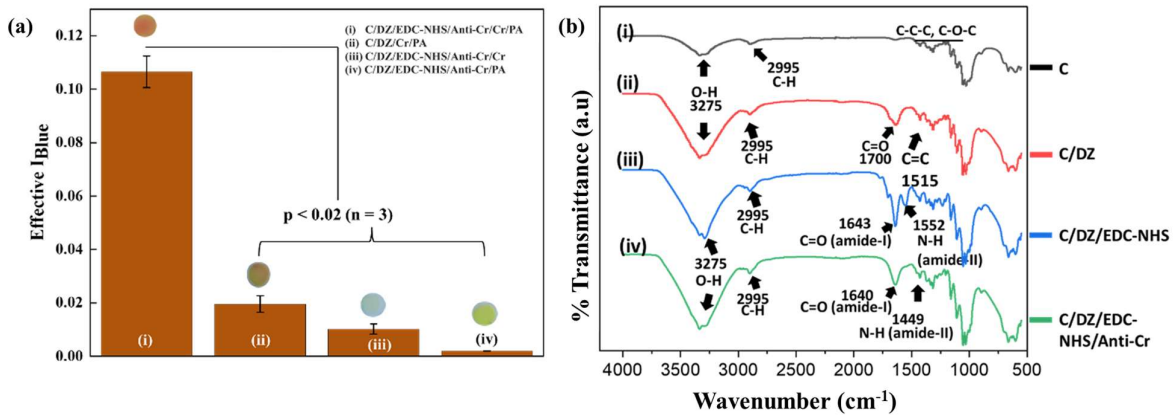

Figure 2.3: (a) *Histograms showing the comparative Effective I_{Blue} of the different sensing probe (i) C/DZ/EDC-NHS/Anti-Cr/Cr/PA, (ii) C/DZ/Cr/PA, (iii) C/DZ/EDC-NHS/Anti-Cr/Cr, and (iv) C/DZ/EDC-NHS/Anti-Cr/PA,* ***(b)*** *FTIR spectra of different stages of probe (i) C, (ii) C/DZ, (iii) C/DZ/EDC-NHS, and (iv)C/DZ/EDC-NHS/Anti-Cr*

The Jaffe reaction, a widely used method for the detection of creatinine, involves the formation of a red-orange creatinine–picrate complex under alkaline conditions. This reaction leads to notable changes in the functional groups of creatinine, which can be monitored using FTIR spectroscopy. Prior to the reaction, the FTIR spectrum of pure creatinine typically exhibits a strong carbonyl (C=O) stretching vibration around 1716 cm^{-1}, N–H bending near 1640 cm^{-1}, broad N–H stretching between 3200–3400 cm^{-1}, and C–N stretching bands around 1317 cm^{-1} (**figure 2.4(a)**). Upon complex formation with picric acid, these characteristic peaks undergo significant changes. The carbonyl stretch often shifts to lower wavenumbers or decreases in intensity due to conjugation with the picrate moiety (**figure 2.4(b)**). These spectral changes confirm the successful interaction between creatinine and picrate and can be used to qualitatively assess complex formation during the Jaffe reaction.

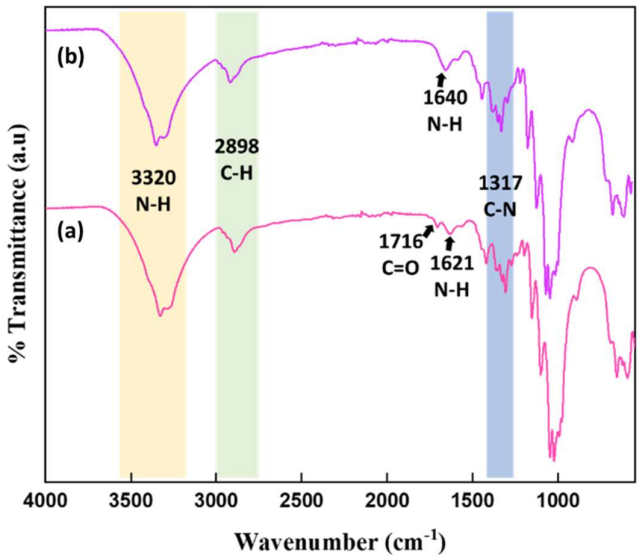

Figure 2.4: *FTIR spectra of sensing probe before and after the final reaction* ***(a)*** *C/DZ/EDC-NHS/Anti-Cr/Cr,* ***(b)*** *C/DZ/EDC-NHS/Anti-Cr/Cr/PA*

Further, AFM was performed to validate the sensor-probe fabrication, where the morphologies of every modified surface have been recorded in the contact mode (**Figure 2.5**). Firstly, the initial surface morphology of the bare cellulose paper (C) was obtained, in which a comparatively smoother topology of the fibrous paper surface appeared with the z-deflection value of 22.3 nm **(Figure 2.5(a))**. After which, the second surface, that was formed by treating the paper surface with 4-carboxybenzene diazonium salt (C/DZ), significant granularity was observed with an increased z-deflection of 46.8 nm, due to conjugation of carboxybenzyl molecules on the surface of cellulose **(Figure 2.5(b))**. In the later stage, when the surface was treated with EDC-NHS to form the C/DZ/EDC-NHS surface, a more significant increase in the z-deflection value of 161.6 nm was recorded **(Figure 2.5(c))**. In the final step of fabrication, upon immobilizing the Anti-Cr, the difference in the surface topology was changed with the increased z-deflection value of 199.4 nm **(Figure 2.5(d))**, which was merely due to the immobilization of Anti-Cr on the C/DZ/EDC-NHS surface. The results from all three

characterization techniques, image analysis (RGB), FTIR, and AFM, complement each other. Therefore, we concluded the successful layer-by-layer synthesis of the sensing probe.

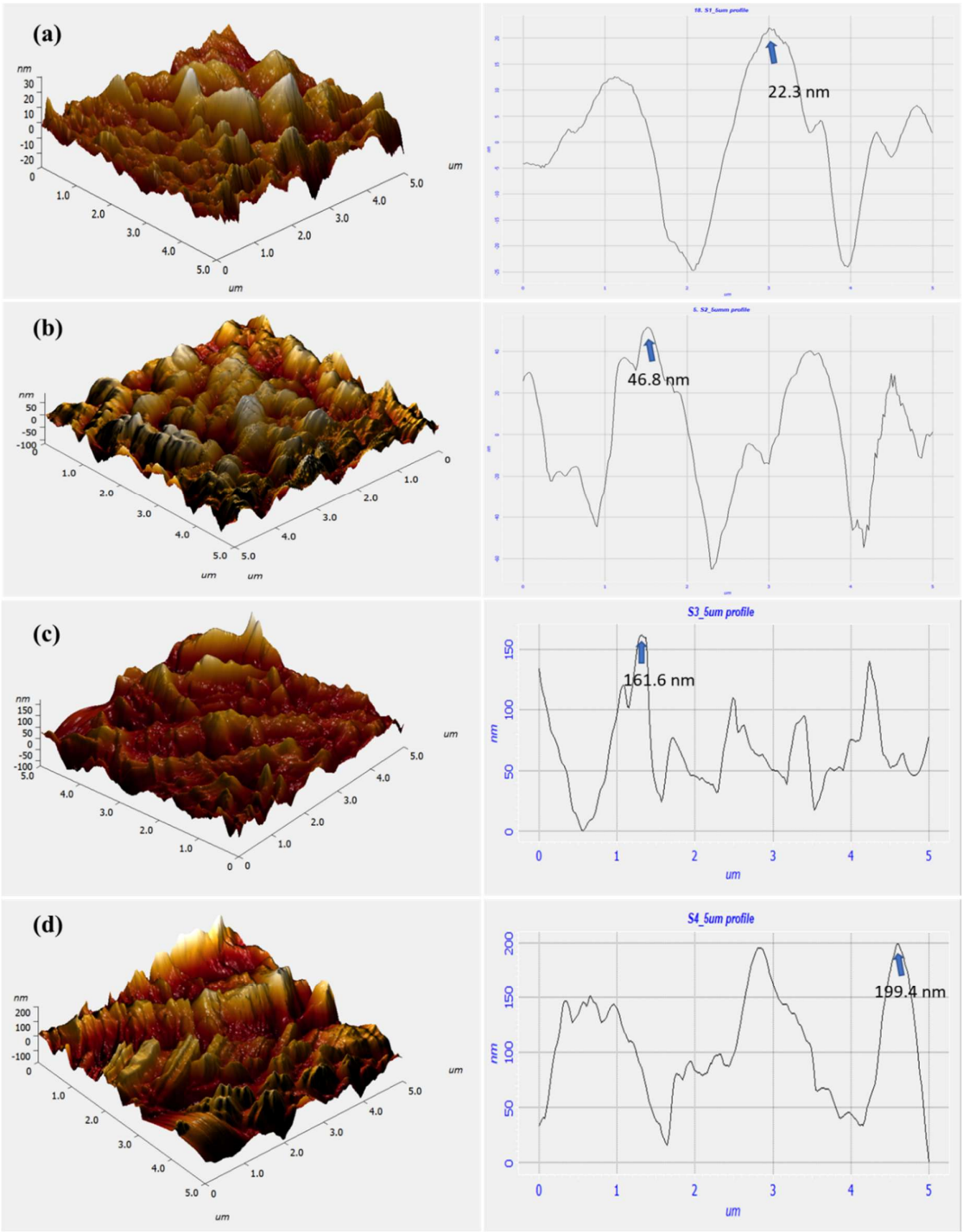

Figure 2.5: *AFM images* ***(a)*** *C (z-deflection – 22.3 nm),* ***(b)*** *C/DZ (z-deflection – 46.8 nm),* ***(c)*** *C/DZ/EDC-NHS (z-deflection – 161.6 nm),* ***(d)*** *C/DZ/EDC-NHS/Anti-Cr (z-deflection – 199.4 nm) representing their z-deflection and micrograph*

3.3. Analytical performance of C/DZ/EDC-NHS/Anti-Cr biosensor

After performing the characterization of the surface of the fabricated sensor probe, its analytical performance needs to be tested and evaluated by measuring the different concentrations of Creatinine. To achieve this, initially, the developed sensing probe was allowed to react with the buffer only in the absence of Creatinine, followed by addition of PA, where no significant Effective I_{Blue} was observed. After that, the developed probe C/DZ/EDC-NHS/Anti-Cr was tested against the different concentrations of Creatinine followed by the reaction with PA, and the change in color was captured using the developed sensing device. **Figure 2.6(a)** displays the Effective I_{Blue} responses of the developed biosensing device in the absence and presence of Creatinine in varying concentrations between 5 and 400 μM. The color change on the probe surface indicates the increase in Effective I_{Blue} values with the increasing concentrations of Creatinine. This proportional change in effective I_{Blue} values with the change in Creatinine concentration has shown that the designed sensing system can effectively and efficiently detect Creatinine. Two different calibration plots with different analytical parameters have been obtained, based on the response of Effective I_{Blue} values. The linear regression equations for Creatinine are represented for low (5 - 20 μM) and high (50 - 400 μM) concentrations calibration plots are as shows: Effective I_{Blue} (a.u.) = 0.049 (± 0.013) + 0.009 (± 0.002) [Cr(μM)] and Effective I_{Blue} (a.u.) = 0.240 (± 0.033) + 0.001 (± 0.001) [Cr(μM)] with adjacent R^2 values of 0.912 and 0.935, respectively. The detection limit of Creatinine was determined to be 0.0146 (± 0.0015) (RSD < 4.7 %) based on the standard deviation obtained from repetitive readings of the blank with a 95.0 % of confidence level, $n = 3$. The obtained detection limit is lower [36] or comparable [37] to the recently reported optical Creatinine sensors. The analytical performance of various sensors in terms of detection time, real sample, detection range, and limit of detection, including sensor configuration has been comprehensively described in **Table 2.1.**

It is worth mentioning that the developed system was able to measure the amount of Creatinine that includes its clinical range in human serum and urine [14,38], hence it can be utilized for routine clinical test in diverse matrices. Interestingly, the detection time of the developed device was recorded to be 7.0 mins which is relatively faster [38] or comparable [39] to the previously reported method.

Table 2.1: *Comparison table of some globally developed creatinine sensor with the developed set up in terms of fabrication, response time, analytical performance (NR: Not Reported)*

S. No.	Detection Method	Sensor Configuration	Time	Real Sample	Dynamic Range	LOD	Ref.
1.	Colorimetric	CuNPs have been integrated with L-cysteine for selective and sensitive interaction with Creatinine	20 min	Serum and Urine	0.33 - 5.33 μM	0.454 nM	[38]
2.	Colorimetric	ABTS was introduced and entrapped in fluorine-doped tin oxide modified chitosan film	12.5 min	Urine	0 - 21300 μM	400 μM	[41]
3.	Colorimetric	3D-printed element was integrated with smartphone for detection using Hue channel intensity in Jaffe method	6 min	Urine	1000 - 2000 μM	350 μM	[39]
4.	Colorimetric	3,5-dinitrobenzoate was used for quantification by targeting green channel	6 min	Urine	820 - 10^5 μM	270 μM	[39]
5.	Fluorescence	Glutathione based copper nanoclusters were designed using ascorbic acid for turn-on mode	15 min	Urine	30 - 1000 μM	13.0 μM	[42]
6.	Optical	C-gold nanocomposite was designed using carbon nanodots derived from *Citrullus lanatus* for photoluminescent imaging	10 min	NR	17 - 1700 μM	6.19 μM	[43]
7.	Optical	H_2O_2 released through Creatinine conversion was detected by reacting it with 4-aminophenazone and hydroxybenzoic acid on a μPAD	15 min	Urine	221 - 2210 μM	176 μM	[36]

8.	Fluorescence	Gluten free gold quantum cluster based turn off - on system	3 hr	Serum	20 - 520 μM	2 nM	[44]
9.	Optical	Silver nanoparticles were capped with 2,2-thiodiacetic acid to react with creatinine	5 min	Serum	0.01 - 1 μM	3 nM	[37]
10.	**Optical**	**C/DZ/EDC-NHS/Anti-Cr/Cr**	**7 min**	**Serum**	**5 - 400 μM**	**0.0146 μM**	**This work**

3.4 Selectivity Assay

To estimate the medical applicability of the designed system, selectivity needs to be tested as it is one of the most critical parameters. Therefore, the selectivity assay was performed with the molecules that are majorly present in the serum matrix, i.e., glucose, bovine serum albumin (BSA), uric acid, citric acid, vitamin C, and commonly present ions (Na^+, K^+, Cl^-) separately, under same experimental conditions. **Figure 2.6(b)** shows the comparative analysis of Effective I_{Blue} values for Creatinine and interfering molecules, in which no change in color and signal was seen for all of the interfering molecules compared to the Creatinine. This happens because of the absence of Creatinine in the measuring solution, which is only responsible for generating a reddish-orange color meditated through PA. Mathematically, the selectivity of the system was determined by calculating the selectivity coefficient (K_{Sel}) using **equation 3**,

$$K_{Sel} = \frac{(Signal)_{interferent}}{(Signal)_{Cr}} \qquad \textit{equation 3}$$

where, K_{Sel} is the selectivity coefficient, $(Signal)_{interferent}$ is the signal value observed when the sensor was checked for the interfering molecules, and $(Signal)_{Cr}$ is the signal observed for the creatinine molecule, with the addition of picric acid.

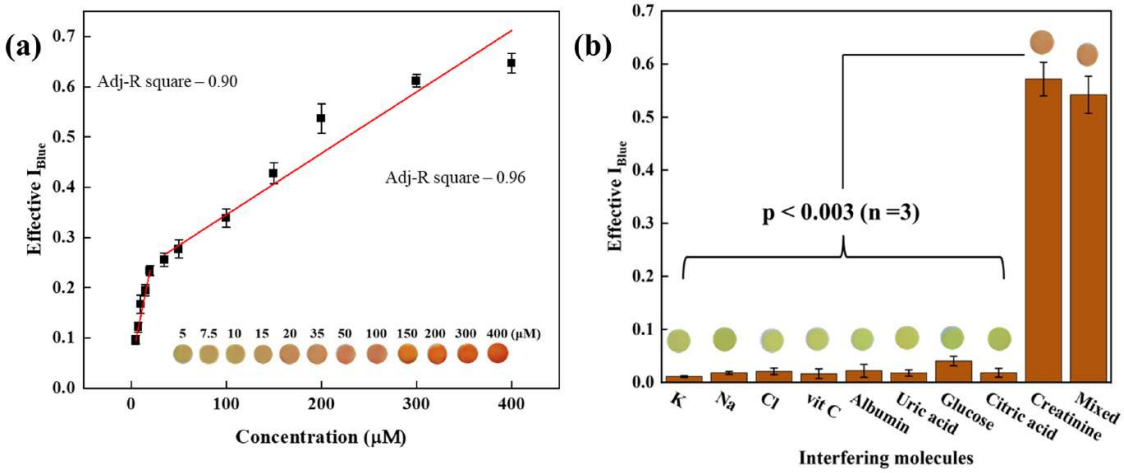

Figure 2.6: (a) *Standard calibration graph showing a linear relationship in the concentration range of Creatinine from 5 - 400 µM,* ***(b)*** *Selectivity assay of C/DZ/EDC-NHS/Anti-Cr sensor probe towards interfering molecules presents in the serum and mixed sample analysis*

It was observed that the k_{sel} for the interfering molecules were less than 1, which indicates that the developed biosensor is highly sensitive and selective towards creatinine, represented in **Table 2.2**. The t-test was also conducted, and the *p*-value was determined for the interfering molecules present in the serum sample against creatinine. The value observed was < 0.003 ($n = 3$), which shows that the readings are statistically insignificant.

Table 2.2: *Description of the obtained Effective I_{Blue} intensity, K_{sel} of the interfering molecules*

S. No.	Interfering molecules	Effective I_{Blue}	K_{sel}
1.	K^+	0.011 (±0.001)	0.019
2.	Na^+	0.018 (±0.002)	0.031
3.	Cl^-	0.021 (±0.006)	0.036
4.	Vitamin C	0.016 (±0.009)	0.028
5.	Albumin	0.022 (±0.012)	0.038
6.	Uric Acid	0.017 (±0.005)	0.029
7.	Glucose	0.042 (±0.009)	0.073
8.	Citric Acid	0.0018 (±0.002)	0.003
9.	Creatinine	0.57 (±0.051)	1

In the serum sample, creatinine is present with the different interfering molecules together; therefore, we have performed mixed sample analysis containing all the molecules with creatinine under similar experimental conditions. To evaluate this, the creatinine was mixed with interfering molecules in the same concentration as in the serum, and the creatinine detection was done using the developed biosensor. In this case, the sensitivity for the creatinine detection was observed to be 94.8 % ($n = 3$) compared to when creatinine was tested separately. Thus, the developed sensor was able to selectively detect the creatinine even in the presence of other molecules, i.e., mixed sample.

3.5. Real sample analysis

The implication of the fabricated biosensing device was validated in serum samples because it is considered as a valuable matrix for diagnosing renal dysfunction [40]. The spike-recovery model was employed for this purpose where the known concentrations of creatinine were added to the serum sample and the signals were compared with the standard calibration plot. The % recovery of creatinine in serum samples was calculated at different concentrations using **equation 4.**

$$\%\ \boldsymbol{Recovery} = \frac{[A]_{Cr} - [B]_{Cr}}{[C]_{Cr}} \times 100 \qquad \textit{equation 4}$$

where, $[A]_{Cr}$ and $[B]_{Cr}$ are the measurements of creatinine in the spiked and blank samples, respectively; and $[C]_{Cr}$ is the amount of creatinine present in the standard solutions.

Figure 2.7 represents a concentration-dependent analytical signal of Creatinine in a serum sample where the proportional increase was observed in Effective I_{Blue} values with the increase in creatinine concentrations. It was also observed that no color change was visible in the sample where no creatinine was added.

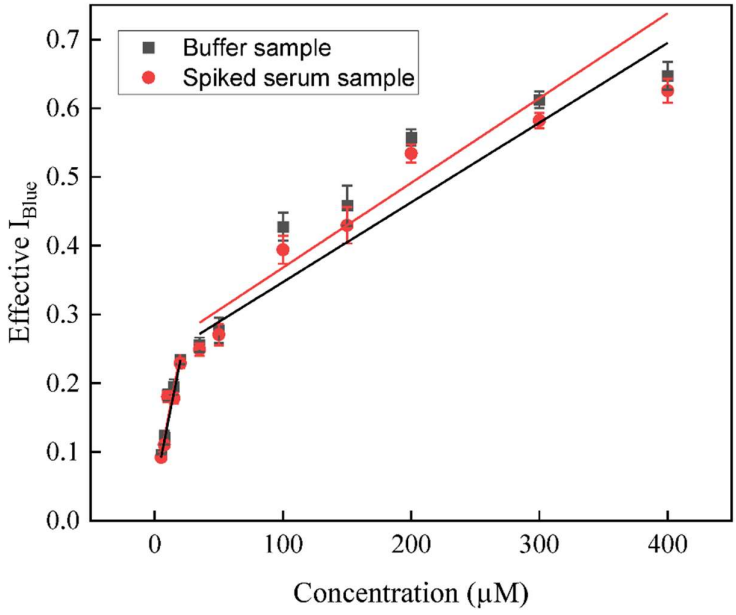

Figure 2.7: *Scatterplot showing the dose-dependent creatinine detection using the sensing probe in standard buffer and spiked serum samples*

Further, to find the sensitivity of the system, the % recovery test was performed and it was found that the sensor was able to quantify the creatinine between 92-98 % from the serum samples. The limit of detection of creatinine in the serum sample was determined to be 0.0342 μM depending upon the standard deviation of three repeated measurements of the blank (95.0% confidence level, *n = 3*). The detailed obtained values are represented in **Table 2.3** showing the recovery % and RSD values. Interestingly the developed probe was tested in real sample where it was observed that developed probe was able to detect target within the clinically relevant range. Such observation represents that the developed sensor system could detect creatinine in serum samples.

Table 2.3: *Recovery table showing percent recoveries of creatinine in spiked serum samples and RSD values*

S. No.	Spiked amount (μM)	Recovered amount (μM)	% Recovery	RSD (%)
1.	5	4.77 (±0.05)	95.40	1.10
2.	7.5	6.75 (±0.18)	90.09	2.80
3.	10	9.54 (±0.25)	95.46	2.66
4.	15	13.45 (±0.26)	89.71	1.96
5.	20	19.46 (±0.39)	97.30	2.02
6.	35	32.99 (±0.99)	94.27	3.02
7.	50	47.31 (±1.41)	94.62	2.98
8.	100	92.55 (±2.92)	92.55	3.15
9.	150	139.99(±4.61)	93.32	3.29
10.	200	189.29(±5.39)	94.64	2.84
11.	300	288.73(±3.62)	96.24	1.25
12.	400	384.50(±4.01)	96.12	1.04

3.6 Storage, stability and reproducibility test

The final sensing probe, i.e., C/DZ/EDC-NHS/Anti-Cr, was stored at 4 °C in a moist environment, and the probe was tested every week for Creatinine detection, and Effective I_{Blue} was recorded. In addition to this, a study for the shelf-life of the designed probe was also done in which the Effective I_{Blue} of the probe was checked after every three days. The results of the Effective I_{Blue} values signify that the sensor system preserves the sensitivity of about 96.5 % up to three weeks, and the decrease in the signal was recorded up to 90.5 (± 1.51) % till the 28th day. The sensing device probe shows up acceptable shelf-life of up to 30 days which is most likely due to the stable immobilization of Anti-Cr and retainment its biological activity during the storage period. It was observed that after 4 weeks, there was a decrease in signal that reached up to 85.6 %. The most probable reason for this decrease in signal was either the reduction of biological activity of Anti-Cr and/or the degradation of the chemical modification steps. Also, the reproducibility was tested for the biosensing device which showed RSD < 4.4% and disc-to-disc RSD was < 3.9 % even when the fabrication was done using the same fabrication steps. These slight variations were observed probably because of the negligible variation during the integrated sensor device designing and some due to handling errors.

4. Device Prototyping and Deployment

The results obtained after all the analysis and testing, including the real samples prove that the developed device prototype is capable of diagnosing chronic kidney disease in a simplified manner by detecting Creatinine in clinical ranges. For translating the device in clinics and personalized uses the device has been fabricated as follows. The device has been designed using a hardboard case as a complete set of dimensions of 8.0 cm (*L*) X 7.5 cm (*W*) X 9.0 cm (*H*), onto which a smartphone is attached, and the test strip was inserted for the detection as shown in **Figure 2.8(a)**. A tunnel-type structure is developed for image acquisition which helps in improving picture sensitivity as the system was not affected by any atmospheric/interfering

light. The dimension of the tunnel structure (3 cm (L) X 3 cm (W) X 9 cm (H)), the strip holder (3.4 cm X 3.4 cm), and the adjustable lens channel are depicted in **Figure 2.8(b)**. This setup assisted in performing the detection and image analysis in one single frame and also helped reduce the need for a controlled laboratory setup, easing the diagnosis process. Also, the paper strip showing the reaction zone (diameter = 5.0 mm) was fabricated, onto which the final probe (C/DZ/EDC-NHS/Anti-Cr) was set up to detect Creatinine**.** This provides a particular spot and allows the reaction to occur in a particular area, which helps in improving the color intensity. The real image of the device performing the detection after the insertion of the test strip has been shown in **Figure 2.8(c)** to show the actual device developed.

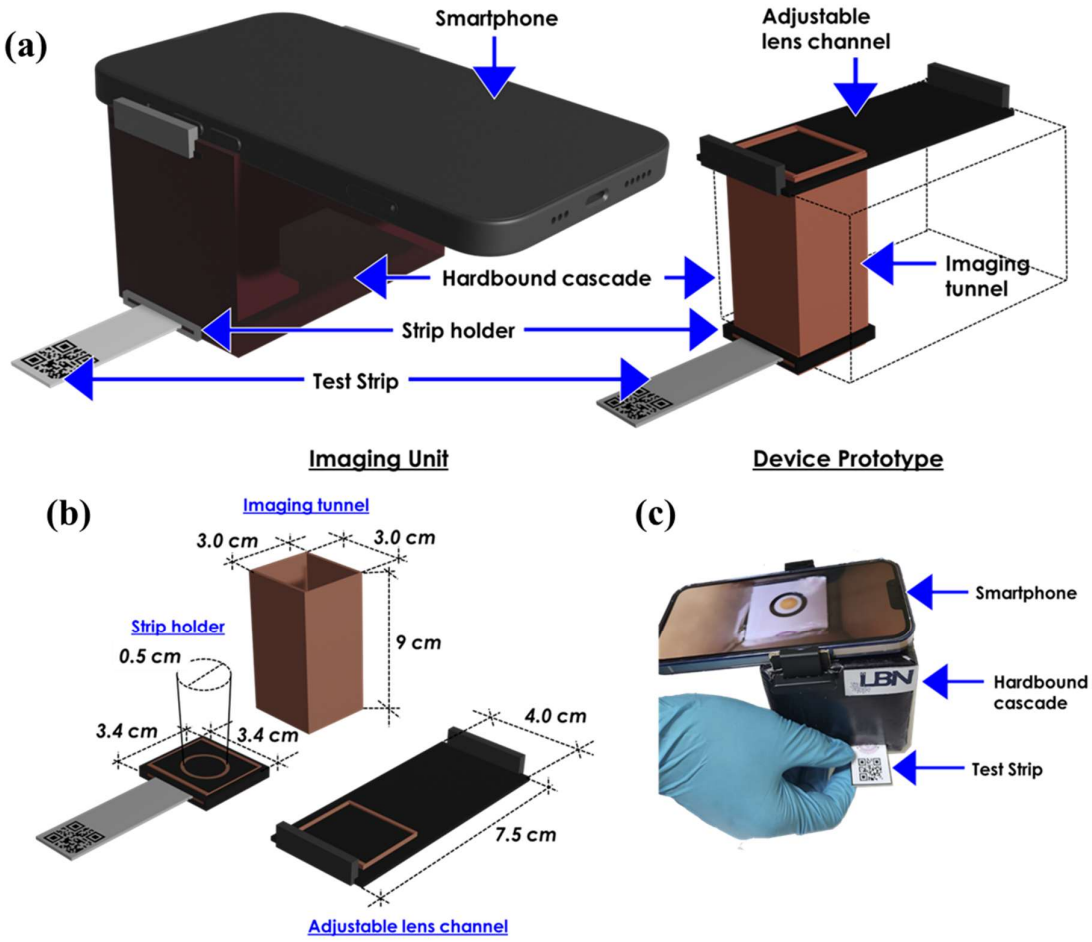

Figure 2.8: (a) *Detailed design of the device setup developed for the creatinine measurement,* ***(b)*** *detailed dimension of the designed tunnel and the strip for image capturing and processing,* ***(c)*** *real image of the developed system taking reading for creatinine detection*

5. Conclusion

A paper-based optical sensor device was developed for point-of-care quantitative monitoring of Creatinine in serum sample. The detection was based on a modified chemical reaction to enhance selectivity and sensitivity. As per our knowledge, this is a first-of-its-kind attempt to make the reaction specific for Creatinine by fabricating a probe that includes Anti-Cr antibody. The change in color was captured, and the image processing was performed based on optical analysis. In this case, change in Effective I_{Blue} values becomes the major factor. It was noted that under optimal conditions, the developed system shows a good linear range of 5- 400 μM, including the clinical range of Creatinine in humans with a limit of detection of 0.0146 μM. Additionally, the developed device shows a highly specific and accurate analytical performance when tested in the serum sample. Further, the probe shows excellent selectivity toward Creatinine in the presence of other proteins and ions in the serum sample. The calculated selectivity of the developed sensor was 94.8 % ($k_{sel} << 1$; $p < 0.003$; $n = 3$) and shows the recovery of 82-98 % in serum samples proving its exceptional potential in the field of medical diagnosis.

References

[1] C.P. Kovesdy, Epidemiology of chronic kidney disease: an update 2022, Kidney Int. Suppl. 12 (2022) 7–11.

[2] P. Cockwell, L.A. Fisher, The global burden of chronic kidney disease, Lancet. 395 (2020) 662–664.

[3] J.C. Lv, L.X. Zhang, Prevalence and Disease Burden of Chronic Kidney Disease, Adv. Exp. Med. Biol. 1165 (2019) 3–15.

[4] I. Lousa, F. Reis, I. Beirão, R. Alves, L. Belo, A. Santos-Silva, New Potential Biomarkers for Chronic Kidney Disease Management-A Review of the Literature, Int. J. Mol. Sci. 22 (2020) 1–37.

[5] R.G. Fassett, S.K. Venuthurupalli, G.C. Gobe, J.S. Coombes, M.A. Cooper, W.E. Hoy, Biomarkers in chronic kidney disease: a review, Kidney Int. 80 (2011) 806–821.

[6] W.R. Zhang, C.R. Parikh, Biomarkers of Acute and Chronic Kidney Disease, Annu. Rev. Physiol. 81 (2019) 309–333.

[7] J. Levy, E. Brown, A. Lawrence, Oxford Handbook of Dialysis, 2016.

[8] I.M. Washington, G. Van Hoosier, Clinical Biochemistry and Hematology, in: Lab. Rabbit. Guinea Pig, Hamster, Other Rodents, 2012.

[9] S. Vupputuri, D.P. Sandler, Lifestyle risk factors and chronic kidney disease, Ann. Epidemiol. 13 (2003) 712–720.

[10] J. Himmelfarb, T.A. Ikizler, Chronic Kidney Disease, Dialysis, and Transplantation: A Companion to Brenner and Rector's The Kidney, 2018.

[11] L.-G. S, M. M, Biomarkers in chronic kidney disease, from kidney function to kidney damage, World J. Nephrol. 4 (2015) 57.

[12] R.B. Kreider, J.R. Stout, Creatine in Health and Disease, Nutrients. 13 (2021) 1–28.

[13] Biomarkers in Acute and Chronic Kidney Diseases - ClinicalKey, (n.d.).

https://www.clinicalkey.com/#!/content/book/3-s2.0-B9780323532655000277

[14] C.S. Pundir, S. Yadav, A. Kumar, Creatinine sensors, TrAC Trends Anal. Chem. 50 (2013) 42–52.

[15] Laboratory Exams For Chronic Kidney Disease - Renal Diet HQ, (n.d.). https://www.renaldiethq.com/laboratory-exams-chronic-kidney-disease/ (accessed October 14, 2022).

[16] Chronic Kidney Disease Tests & Diagnosis | NIDDK, (n.d.). https://www.niddk.nih.gov/health-information/kidney-disease/chronic-kidney-disease-ckd/tests-diagnosis (accessed October 14, 2022).

[17] N. Tajarrod, M.K. Rofouei, M. Masteri-Farahani, R. Zadmard, A quantum dot-based fluorescence sensor for sensitive and enzymeless detection of creatinine, Anal. Methods. 8 (2016) 5911–5920.

[18] A.H. Aly, D. Mohamed, M. A. Mohaseb, N.S.A. El-Gawaad, Y. Trabelsi, Biophotonic sensor for the detection of creatinine concentration in blood serum based on 1D photonic crystal, RSC Adv. 10 (2020) 31765–31772.

[19] S. Kalasin, P. Sangnuang, P. Khownarumit, I.M. Tang, W. Surareungchai, Evidence of Cu(I) Coupling with Creatinine Using Cuprous Nanoparticles Encapsulated with Polyacrylic Acid Gel-Cu(II) in Facilitating the Determination of Advanced Kidney Dysfunctions, ACS Biomater. Sci. Eng. 6 (2020) 1247–1258.

[20] U. Lad, S. Khokhar, G.M. Kale, Electrochemical creatinine biosensors, Anal. Chem. 80 (2008) 7910–7917.

[21] S. Ekelund, P. Paby, High-performance liquid chromatographic determination of creatinine, Scand. J. Clin. Lab. Invest. 51 (1991) 67–71.

[22] M. Fernández-Fernández, P. Rodríguez-González, M.E. Añón Álvarez, F. Rodríguez, F. V. Álvarez Menéndez, J.I. García Alonso, Simultaneous determination of creatinine and

creatine in human serum by double-spike isotope dilution liquid chromatography-tandem mass spectrometry (LC-MS/MS) and gas chromatography-mass spectrometry (GC-MS), Anal. Chem. 87 (2015) 3755–3763.

[23] B. Purohit, P.R. Vernekar, N.P. Shetti, P. Chandra, Biosensor nanoengineering: Design, operation, and implementation for biomolecular analysis, Sensors Int. 1 (2020) 100040.

[24] P. Chandra, R. Prakash, Nanobiomaterial engineering: Concepts and their applications in biomedicine and diagnostics, Nanobiomaterial Eng. Concepts Their Appl. Biomed. Diagnostics. (2020) 1–294.

[25] R.W. Bonsnes, H.H. Taussky, on the colorimetric determination of creatinine by the jaffe reaction, J. Biol. Chem. 158 (1945) 581–591.

[26] J. Siedel, R. Deeg, H. Seidel, H. Mollering, J. Staepels, H. Gauhl, J. Ziegenhorn, Fully Enzymatic Colorimetric Assay of Serum and Urine Creatinine Which Obviates the Need for Sample Blank Measurements, Http://Dx.Doi.Org/10.1080/00032718808071927. 21 (2006) 1009–1017.

[27] M.L. Sin, K.E. Mach, P.K. Wong, J.C. Liao, Advances and challenges in biosensor-based diagnosis of infectious diseases, Expert Rev. Mol. Diagn. (2014).

[28] K. Mahato, A. Srivastava, P. Chandra, Paper based diagnostics for personalized health care: Emerging technologies and commercial aspects, Biosens. Bioelectron. 96 (2017) 246–259.

[29] K. Mahato, P. Chandra, Paper-based miniaturized immunosensor for naked eye ALP detection based on digital image colorimetry integrated with smartphone, Biosens. Bioelectron. 128 (2019) 9–16.

[30] K. Mahato, B. Purohit, A. Kumar, P. Chandra, Paper-based biosensors for clinical and biomedical applications: Emerging engineering concepts and challenges, Compr. Anal. Chem. 89 (2020) 163–188.

[31] S. Natarajan, M.C. Derosa, M.I. Shah, J. Jayaraj, Development and Evaluation of a Quantitative Fluorescent Lateral Flow Immunoassay for Cystatin-C, a Renal Dysfunction Biomarker, Sensors (Basel). 21 (2021).

[32] G. de Carvalho Oliveira, C.C.S. Machado, D.K. Inácio, J.F. da Silveira Petruci, S.G. Silva, RGB color sensor for colorimetric determinations: Evaluation and quantitative analysis of colored liquid samples, Talanta. 241 (2022) 123244.

[33] H.J. Chun, Y.D. Han, Y.M. Park, K.R. Kim, S.J. Lee, H.C. Yoon, An Optical Biosensing Strategy Based on Selective Light Absorption and Wavelength Filtering from Chromogenic Reaction, Mater. 2018, Vol. 11, Page 388. 11 (2018) 388.

[34] J. Saha, S.Y. Wang, A.J. Davis, Examining DNA Double-Strand Break Repair in a Cell Cycle-Dependent Manner, Methods Enzymol. 591 (2017) 97–118.

[35] Y. Ji, X. Yang, Z. Ji, L. Zhu, N. Ma, D. Chen, X. Jia, J. Tang, Y. Cao, DFT-Calculated IR Spectrum Amide I, II, and III Band Contributions of N-Methylacetamide Fine Components, ACS Omega. 5 (2020) 8572–8578.

[36] K. Talalak, J. Noiphung, T. Songjaroen, O. Chailapakul, W. Laiwattanapaisal, A facile low-cost enzymatic paper-based assay for the determination of urine creatinine, Talanta. 144 (2015) 915–921.

[37] S. Mohammadi, G. Khayatian, Highly selective and sensitive photometric creatinine assay using silver nanoparticles, Microchim. Acta. 182 (2015) 1379–1386.

[38] U. Sivasankaran, T.C. Jos, K. Girish Kumar, Selective recognition of creatinine – Development of a colorimetric sensor, Anal. Biochem. 544 (2018) 1–6.

[39] I. Lewińska, M. Speichert, M. Granica, Ł. Tymecki, Colorimetric point-of-care paper-based sensors for urinary creatinine with smartphone readout, Sensors Actuators B Chem. 340 (2021) 129915.

[40] A. Forbes, H. Gallagher, Chronic kidney disease in adults: Assessment and

management, Clin. Med. J. R. Coll. Physicians London. (2020).

[41] D.S. Ciou, P.H. Wu, Y.C. Huang, M.C. Yang, S.Y. Lee, C.Y. Lin, Colorimetric and amperometric detection of urine creatinine based on the ABTS radical cation modified electrode, Sensors Actuators B Chem. 314 (2020) 128034.

[42] S. Thammajinno, C. Buranachai, P. Kanatharana, P. Thavarungkul, C. Thammakhet-Buranachai, A copper nanoclusters probe for dual detection of microalbumin and creatinine, Spectrochim. Acta Part A Mol. Biomol. Spectrosc. 270 (2022) 120816.

[43] P.J. Babu, A.M. Raichur, M. Doble, Synthesis and characterization of biocompatible carbon-gold (C-Au) nanocomposites and their biomedical applications as an optical sensor for creatinine detection and cellular imaging, Sensors Actuators B Chem. 258 (2018) 1267–1278.

[44] M.S. Mathew, K. Joseph, Green Synthesis of Gluten-Stabilized Fluorescent Gold Quantum Clusters: Application As Turn-On Sensing of Human Blood Creatinine, ACS Sustain. Chem. Eng. 5 (2017) 4837–4845.